

## Zein Film: Effects of Dielectric Barrier Discharge Atmospheric Cold Plasma

S. K. Pankaj,<sup>1</sup> Carmen Bueno-Ferrer,<sup>1</sup> N. N. Misra,<sup>1</sup> Paula Bourke,<sup>1</sup> P. J. Cullen<sup>1,2</sup>

<sup>1</sup>BioPlasma Research Group, School of Food Science and Environmental Health, Dublin Institute of Technology, Cathal Brugha Street, Dublin 1, Ireland

<sup>2</sup>School of Chemical Engineering, UNSW Australia, Sydney, New South Wales 2052 Australia

Correspondence to: P. Cullen (E-mail: [pjcullen@dit.ie](mailto:pjcullen@dit.ie))

**ABSTRACT:** Dielectric barrier discharge atmospheric plasma is a novel nonthermal technology for the food and packaging industry. The effects of dielectric barrier discharge plasma on the surface, structural, thermal, and moisture sorption properties of edible zein films have been examined. Plasma treatment increased the surface roughness and equilibrium moisture content of the zein film in a direct relationship with the applied voltage level. No significant difference in the thermal stability of the zein film is also observed after plasma treatment. Dielectric barrier discharge plasma treatments of zein film lead to a change in the protein conformation which is confirmed by X-ray diffraction and Fourier transform Infrared spectroscopy. The evaluation of films modifications by plasma discharge will contribute to enhance the in-package decontamination studies of food products by plasma. © 2014 Wiley Periodicals, Inc. *J. Appl. Polym. Sci.* **2014**, *131*, 40803.

**KEYWORDS:** biodegradable; biopolymers and renewable polymers; morphology

Received 4 February 2014; accepted 1 April 2014

DOI: [10.1002/app.40803](https://doi.org/10.1002/app.40803)

### INTRODUCTION

Biodegradable polymers from renewable resources have shown significant potential in packaging applications due to their environmental benefits. While biodegradable packaging materials have limitations pertaining to properties and cost, the fact that certain chemicals used for synthetic packaging are endocrine disruptors and lead to greenhouse gases, the demand for eco-friendly wrappings has increased.<sup>1,2</sup> Zein, is a primary byproduct of the bioethanol industry thus justifying its practicality for efficient utilization of green biomass.

Zein was first described by John Gorham in 1821 after isolating the protein from corn and in 1909, the first patent was granted for preparing plastic from zein.<sup>3,4</sup> Zein is a water-insoluble prolamins present in corn endosperm cells with a high content of hydrophobic amino acids (leucine, proline, and alanine).<sup>5</sup> Zein can be cast into films by dissolving it in a hydrated organic solvent, such as ethanol or acetone, and then drying.<sup>6</sup> However, films made of 100% zein are brittle, therefore plasticizers are added to improve flexibility.<sup>7</sup> Zein films are distinctive as they are tough, glossy, hydrophobic, greaseproof, and resistant to microbial attack ensuring its suitability as coatings, fibers, and packaging films for food and pharmaceutical industries.<sup>5,8</sup> The effectiveness of using zein films as edible coating for maintain-

ing post-harvest quality has been demonstrated for produce including; apple, broccoli, and tomato.<sup>9–11</sup>

Recently, Atmospheric Cold Plasma (ACP) has gained attention for the decontamination of fresh fruits and vegetables.<sup>12–14</sup> ACP is characterized by the disequilibrium of temperature between electrons and ions and can be generated by various methods.<sup>15</sup> Dielectric barrier discharge (DBD) is one of the common methods to generate ACP. In most common DBD devices, plasma is generated between two plane-parallel metal electrodes among which at least one of the electrodes is covered by a dielectric layer. A filamentary discharge is formed by micro-discharges or streamers, which develop on the dielectric layer surface. The dielectric layer plays an important role in limiting the discharge current to avoid an arc transition and to randomly distribute streamers on the electrode surface resulting a homogeneous treatment.<sup>16</sup> DBD plasma is well known for the modification of both the surface and bulk properties of polymers.<sup>17</sup> The effects of DBD plasma on conventional polymers like polyethylene, polypropylene, poly(ethylene terephthalate), and polystyrene have been reported but there is limited information available on the effects of DBD plasma on biodegradable polymers.<sup>18–22</sup> The aim of this work is to characterize the effects of DBD ACP plasma treatments on surface, structural, thermal, and moisture sorption properties of biodegradable corn zein films.

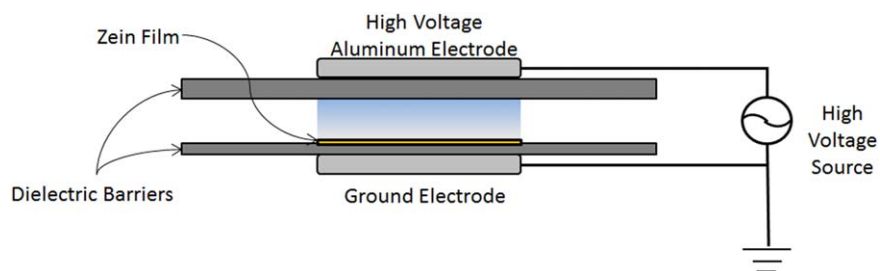


**Figure 1.** Schematic of the experimental setup for DBD plasma system. [Color figure can be viewed in the online issue, which is available at wileyonlinelibrary.com.]

## EXPERIMENTAL

### Materials

Zein films were prepared as described by Mastromatteo, Barbuzzi, Conte, and Del Nobile<sup>23</sup> with slight modifications. Five grams of zein (Sigma-Aldrich, Ireland) were dissolved into 26 mL of 95% ethanol at 50°C. Three grams of glycerol (Sigma-Aldrich, Ireland) were added to the solution and stirred using a hotplate magnetic stirrer for 10 min. The film forming solutions were poured on Petri dishes (diameter 15 cm) and dried at ambient conditions under laminar flow hood until the solvent was completely evaporated and peeled off after 48 h. The cast zein films had an average thickness of  $385 \pm 10 \mu\text{m}$ .

### Plasma Treatment

A schematic of the experimental setup is presented in Figure 1. The DBD plasma source consists of two circular aluminum

plate electrodes (outer diameter = 158 mm) over perspex dielectric layers (10 mm thickness). The applied voltage to the electrode was obtained from a step-up transformer (Phenix Technologies, USA). The input voltage to the primary winding was 230V at a frequency of 50 Hz. A 2-mm-thick polypropylene sheet was used to stabilize the discharge. The distance between electrodes was 22 mm. The atmospheric air conditions at the time of treatment were 48% relative humidity (RH) and 20°C. The samples were treated at 60, 70, and 80 kV for 1, 2, 3, 4, and 5 min.

### Material Characterization

**Atomic Force Microscopy (AFM).** AFM measurements were carried out to observe the surface topography of the samples before and after DBD plasma treatment. The AFM used was MFP-3D BIO 1126 (Asylum Research, Santa Barbara, CA)

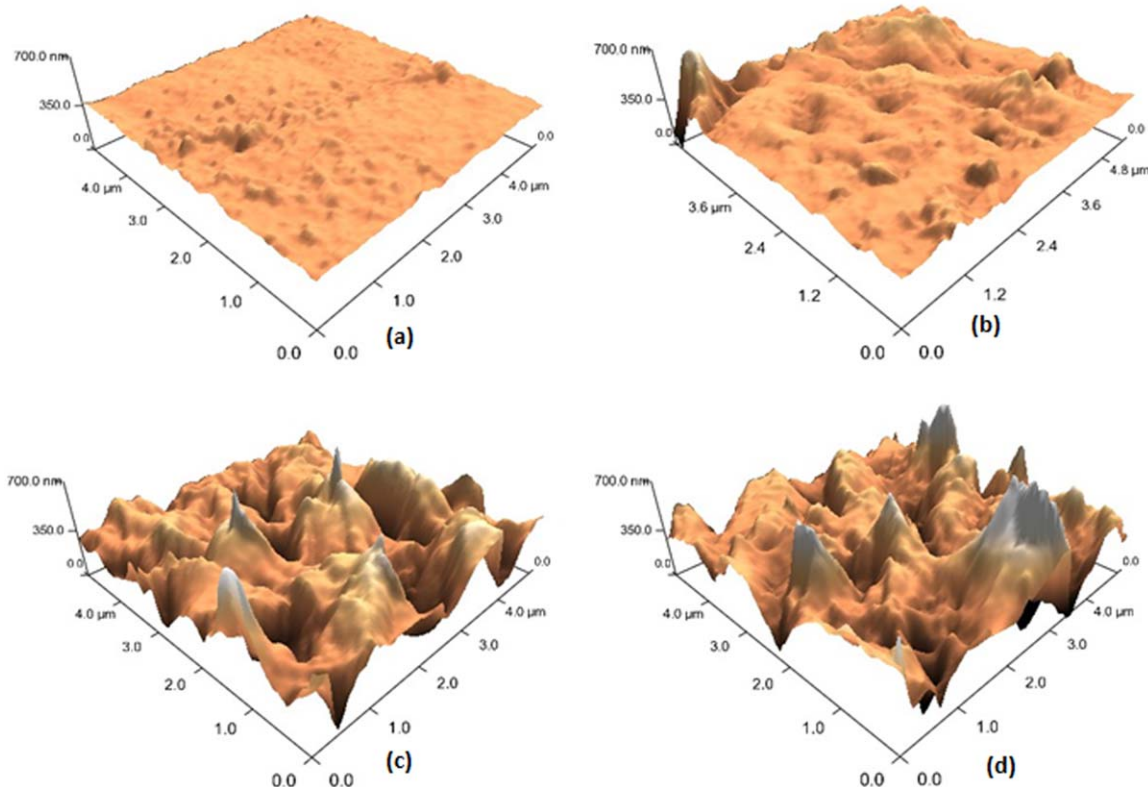


**Figure 2.** AFM images of the surface of untreated and plasma-treated cast zein films. (a) Untreated, (b) 60 kV–5 min, (c) 70 kV–5, (d) 80 kV–5. [Color figure can be viewed in the online issue, which is available at wileyonlinelibrary.com.]

**Table I.** Roughness Parameters for Control and DBD Plasma-Treated Cast Zein Films ( $R_{\text{RMS}}$ , Root Mean Square Roughness (Mean Value);  $R_{\text{Peak}}$ , Highest peak,  $R_{\text{Groove}}$ , Lowest Groove)

Voltage (kV)	Time (min)	$R_{\text{RMS}}$ (nm)	$R_{\text{Peak}}$ (nm)	$R_{\text{Groove}}$ (nm)
Control		16.410	125.991	66.995
60	5	52.044	295.146	337.616
70	5	126.164	496.313	506.472
80	5	132.869	641.017	651.892

operated in intermittent contact (tapping) mode. The images were collected at a fixed scan rate of 0.5 Hz. The sampling rate was 512 lines. The data was processed using MF3D software (version 111111 + 1219).

**Water Sorption Kinetics.** Water sorption kinetics was determined by the method of Pereda, Aranguren and Marcovich.<sup>24</sup> Briefly, the films were dried at 40°C for 3 days in a vacuum oven at 500 mm pressure at 25°C. After drying, films were DBD plasma treated and placed in a versatile environmental test chamber (Model MLR-350H, Sanyo Electric Biomedical, Japan) at a controlled humidity environment of 75% at 23°C. Samples were weighed gravimetrically at equal time intervals with a precision of  $\pm 0.0001$  g. This experiment was performed in triplicate to ensure the reproducibility of the results. The moisture content ( $M_t$ ) of films as a function of time was obtained from the total mass balance of the sample as a function of time as given in eq. (1).

$$M_t(\%) = \frac{(W_t - W_0) \times 100}{W_0} \quad (1)$$

where  $M_t$  = moisture content of the sample at time  $t$  (%),  $W_t$  = weight of the sample at time  $t$  (g),  $W_0$  = initial dry weight of sample (g).

**Thermogravimetric Analysis (TGA).** TGA analysis was performed with a DTG-60 instrument (Shimadzu, Ireland). Samples were heated at 10°C min<sup>-1</sup> from room temperature to 700°C under nitrogen atmosphere (flow rate 50 mL min<sup>-1</sup>). The initial degradation temperature ( $T_5$ ) was determined as the temperature at which 5% of mass was lost.

**Differential Scanning Calorimetry (DSC).** DSC analysis was performed with a Differential Scanning Calorimeter DSC2010 with a refrigerating cooling system (RCS) (TA Instruments, AGB Scientific, Dublin, Ireland) under a dry nitrogen gas flow rate of 50 mL min<sup>-1</sup>. Approximately 3 mg samples were

weighed in aluminum pans (40  $\mu$ L) and subjected to heating-cooling cycles from -30°C to 200°C at 10°C min<sup>-1</sup>. Glass transition temperatures ( $T_g$ ) and melting endotherm were determined in the first heating scan.

**X-ray Diffraction (XRD).** Wide-angle X-ray scattering (WAXS) was performed on a Bruker D8-Advance (USA) diffractometer, equipped with a Cu-K $\alpha$  radiation source ( $\lambda = 1.546\text{\AA}$ ), operating at 40 kV and 40 mA as the applied voltage and current, respectively. The incidence angle ( $2\theta$ ) was varied between 5° and 90° at a scanning rate of 2° min<sup>-1</sup>.

**Fourier Transform Infrared Spectroscopy (FTIR).** FTIR spectroscopy was carried out by using a Perkin Elmer FTIR/FTNIR spectrometer (Spectrum 400) from 4000 to 400 cm<sup>-1</sup> to measure any changes in the spectra intensities. A background spectrum was collected by keeping the resolution as 4 cm<sup>-1</sup>. After the background scan, treated and untreated film samples were placed in the sample holder and analyzed.

## RESULTS AND DISCUSSIONS

### Surface Properties

DBD plasma is known for increasing the surface roughness of polymers due to the etching effect. Etching by DBD plasma can be due to chemical (breaking of bonds, chain scission, chemical degradation) or physical processes (physical removal of low molecular fragments).<sup>25-27</sup> The possibility of a change in surface roughness resulting from micro-discharge filaments cannot be also completely overruled. The AFM topography of the zein surface is shown in Figure 2 and the roughness parameters are shown in Table I. It is evident that DBD plasma treatment increased the surface roughness of the zein film. Surface roughness was observed to be increasing with an increase in the applied voltage and treatment time. Similar increases in the surface roughness after plasma treatment have also been reported for common polymers such as; low-density polyethylene, polypropylene, poly(ethylene terephthalate), and poly(lactic acid).<sup>19,28-30</sup>

### Water Sorption Kinetics

Generally, protein films have poor moisture barrier properties due to their hydrophilic nature. Use of glycerol as plasticizer further increases the moisture sorption capacity due to its hydrophilic nature as shown by Lawton<sup>31</sup> and Wei and Baianu.<sup>32</sup> Water diffusion into hydrophilic polymers is associated with relaxation of the polymer chain and an increase in the free volume. There are many empirical and fundamental models proposed in the literature for the absorption of water in hydrophilic films. In this study the Peleg equation was chosen

**Table II.** Fitting Parameters of the Peleg Equation and Fickian Model for DBD Plasma-Treated Zein Films

Treatments	Peleg Equation			Fickian Model		
	$K_1$ (min/wt %)	$K_2$ (wt % <sup>-1</sup> )	RMSE	$M_{\text{eq}}$ (%)	$D$ (cm <sup>2</sup> /s)	RMSE
Control	19.51	0.082	0.84	10.43	$6.85 \times 10^{-9}$	1.246
60 kV/5 min	17.06	0.062	1.11	13.95	$5.81 \times 10^{-9}$	1.709
70kV/5 min	11.86	0.052	0.99	16.93	$6.63 \times 10^{-9}$	1.602
80 kV/5 min	8.994	0.046	0.72	19.18	$7.64 \times 10^{-9}$	1.472

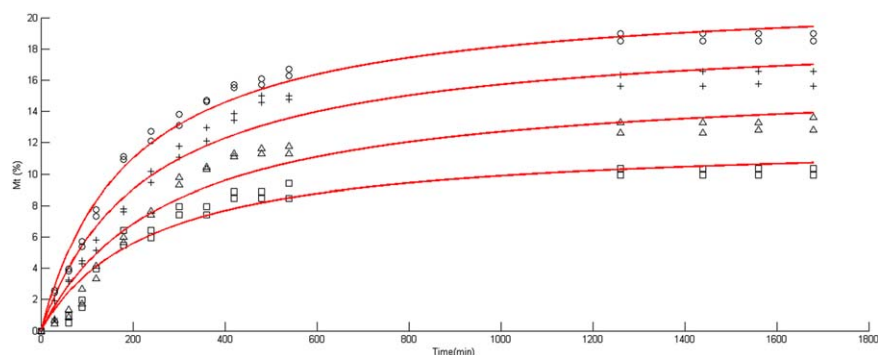


**Figure 3.** Moisture sorption of zein films after DBD plasma treatment at 23°C and 75% RH (solid lines represent the fitting from the Peleg equation, Control(□), 60 kV–5 min(Δ), 70 kV–5 min(+), 80 kV–5 min(O). [Color figure can be viewed in the online issue, which is available at wileyonlinelibrary.com.]

for the empirical description of the sorption process. This equation relates the moisture content at a given time ( $M_t$ ) with the initial moisture content ( $M_0$ ) as given in eq. (2).

$$M_t = M_0 + \frac{t}{K_1 + K_2 \cdot t} \quad (2)$$

where  $t$  is time (min) and  $K_1$  and  $K_2$  are fitting parameters.  $K_1$  is Peleg's rate factor (min/wt %) and is associated with the initial absorption rate,  $K_2$  is Peleg's capacity parameter (wt %<sup>-1</sup>) and is related to the final absorption capacity.

As a fundamental model describing the water absorption on films, Fick's second law intended for a plane sheet with constant boundary conditions and uniform initial concentration was used as reported in eq. (3).

$$M(t) = M_{eq} \left[ 1 - \frac{8}{\pi^2} \sum_{n=0}^{\infty} \frac{1}{(2n+1)^2} \cdot \exp \left\{ \frac{-D \cdot (2n+1)^2 \cdot \pi^2 \cdot t}{h^2} \right\} \right] \quad (3)$$

where  $M(t)$  is the moisture content (%) at time  $t$  (s),  $M_{eq}$  is the moisture at equilibrium conditions (%),  $D$  is the diffusion coefficient (cm<sup>2</sup> s<sup>-1</sup>) through the swollen polymeric matrix and  $h$  is the film thickness (cm).

Experimental moisture sorption data were fitted with the Peleg equation and Fick's diffusion model and the fitting parameters are reported in Table II (Figure 3). An increase in the equilibrium moisture content was observed after the DBD plasma treatment. This increase was found to be directly correlated with the treatment voltage. For the control film the equilibrium moisture content was 10.2% while after plasma treatment at 80 kV for 5 min, it increased to 18.7%. In this study the Peleg equation was found to describe the process better than the Fickian model as evident from the root mean square error (RMSE) values. This can be explained by the fact that, Fick's model describes mass transport related to Brownian motions in which the penetrant flow is exclusively driven by a concentration gradient while water sorption in moderately hydrophilic polymers is a complex phenomenon due to the presence of specific interactions between water molecules and the hydrophilic sites on the polymer backbone.<sup>24</sup> The system of DBD plasma discharge employed is a potential source of reactive oxygen (ROS) and reactive nitrogen species (RNS) which has been reported in previous studies.<sup>25</sup> An increase in the surface oxygenation after plasma treatment has been observed by many

authors leading to an increase in the hydrophilicity of the sample.<sup>17</sup> This increase in the hydrophilicity can be correlated with the increased equilibrium moisture content of the films.

### Thermal Properties

The initial degradation temperature of zein film was not significantly ( $P > 0.05$ ) different after DBD plasma treatment. The  $T_5$  for untreated control zein film was 148.1°C while after plasma treatment it was in the range of 146.3°C to 150.6°C. The initial step of mass loss for control film was found in the region of 78°C while after plasma treatment it was in the region of 82 to 93°C which also suggests the increase in water retention capacity of the zein film after plasma treatment. The results were different than the studies conducted on commercial biodegradable polymer like poly (lactic acid) where an increased thermal stability was observed.<sup>30</sup>

In the DSC thermogram, no significant change was observed in  $T_g$  after plasma treatment and the values are in good agreement with other studies using glycerol as plasticizer.<sup>31,33</sup> This implies that glycerol was effectively incorporated, by penetrating the protein network, forming hydrogen bonds with the protein molecules and thus increasing the separation between the protein chains. However, ACP treatment clearly changed the

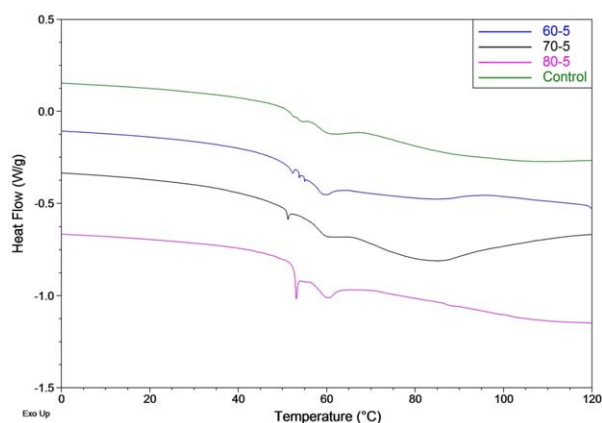


**Figure 4.** DSC thermogram of DBD plasma-treated zein films. A, B: Voltage (kV)-Treatment time (min). [Color figure can be viewed in the online issue, which is available at wileyonlinelibrary.com.]

pattern of thermograms of the plasticized zein films, since an endothermic event between 50 and 55°C appears in all the treated samples, but it is not distinguishable in the control sample. This phenomenon was evident in the samples subjected to 5 min of treatment time (Figure 4). It is also noted that as voltage increases, enthalpies associated with this event are higher and peak shapes also differ, with three small peaks for samples treated at 60 kV and one well-defined peak for sample treated at 80 kV observed. Given the fact that this event appears just before the glass transition in all the samples, it could be attributed to a breakdown of cross-linkages leading to a reorganization of the protein conformational structure as the molecules obtain sufficient freedom of motion.

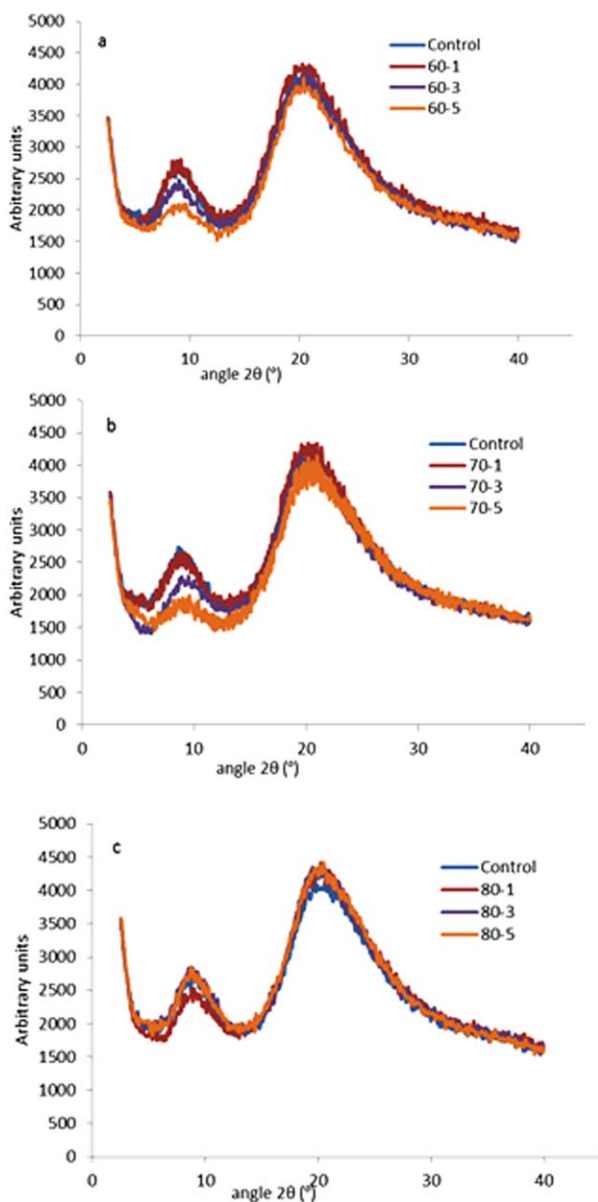


**Figure 5.** X-ray diffractogram of zein film after DBD plasma treatment at (a) 60 kV (b) 70 kV, and (c) 80 kV. [Color figure can be viewed in the online issue, which is available at [wileyonlinelibrary.com](http://wileyonlinelibrary.com).]

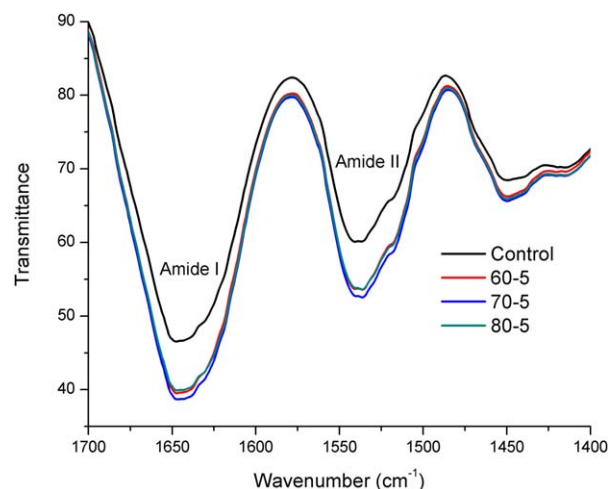


**Figure 6.** FTIR spectra of DBD plasma treated and control zein films in amide I and amide II region. A, B: Voltage (kV)-Treatment time (min). [Color figure can be viewed in the online issue, which is available at [wileyonlinelibrary.com](http://wileyonlinelibrary.com).]

### X-ray Diffraction (XRD)

The WAXS pattern of zein films is shown in Figure 5. Two broad peaks appear in all the diffractograms at  $2\theta = 8.7$  and  $2\theta = 19.3$ . By applying Bragg's law, distances of 10.1 Å and 4.6 Å respectively were calculated. The smaller distance (4.6 Å) corresponds to the average backbone distance within the  $\alpha$ -helix. The larger distance (10.1 Å) is related to the lateral  $\alpha$ -helix packing or the mean distance among neighboring helices.<sup>33–35</sup> As evident from Figure 6(a,b), after ACP treatment of zein films at 60 kV and 70 kV there is a decrease in the intensity of the first peak. Since the 10.1 Å is related to the inter-helix packing, the decline of intensity implies the disruption of zein molecular aggregates, which was also observed by Wang, Geil and Padua<sup>34</sup> with the application of higher mechanical energy during film processing. At 80 kV, the reduction of the first peak's intensity was only observed after 1 minute of treatment. The second spacing corresponding to 4.6 Å (peak at  $2\theta = 19.3$  in Figure 6) was clearly less affected in all the plasma-treated samples, suggesting that the helical configuration of zein was not disturbed by plasma treatment.

### Fourier Transform Infrared Spectroscopy (FTIR)

In the amide I region, band around  $1650\text{ cm}^{-1}$  can be assigned to  $\alpha$ -helical and disordered conformation (stretching vibrations of the C=O bond of the amide) and the band at  $1685\text{ cm}^{-1}$  is due to  $\beta$ -sheets.<sup>36</sup> A broad peak was observed around  $1650\text{ cm}^{-1}$ , which is consistent with an  $\alpha$  helical structure (Figure 6). The increase of intensity observed at this band after DBD plasma treatment suggests that the ACP treatment increased the amount of  $\alpha$ -helical and disordered conformations. The result is in agreement with the DSC thermograms and XRD diffractogram which also suggested a change in the protein conformation after plasma treatment. An increase in the intensity of amide II band at  $1540\text{ cm}^{-1}$  (bending vibrations of the N—H bond) after DBD plasma treatment was also observed. This change may be due to two main factors (i) more extensive hydrogen bonding between the protein, reducing the number of

nonbonded peptide groups and (ii) a shift from  $\beta$ -sheet structure, which absorbs around  $1525\text{ cm}^{-1}$ , to  $\alpha$ -helical structure, which has its amide II maximum at  $1545\text{ cm}^{-1}$ .<sup>37</sup> Bands were also observed at the  $2800\text{--}3000\text{ cm}^{-1}$  range,  $1447\text{ cm}^{-1}$ , and  $720\text{ cm}^{-1}$  which are attributed to the vibrations of attached hydrocarbon chains.<sup>38</sup>

## CONCLUSIONS

DBD plasma treatment of zein film increases the surface roughness of the film. It also increases the equilibrium moisture content of the film. No significant difference in the thermal stability of zein was also observed for all the voltage levels and treatment times. ACP treatment led to a reorganization of the protein conformational structure as evident from the DSC and XRD results. FTIR spectrum also confirms the changes in the amide I and amide II region after plasma treatment. The use of different voltages and treatment times for specific food-package systems could be a promising environmentally friendly alternative to tailor a stable in-package decontamination method using edible zein films. Further studies are suggested to understand the impact of these ACP induced changes on the packaging suitability of the zein film and ultimately on the shelf-life of food products.

## REFERENCES

1. Isobe, S. *Farming Jpn.* **2003**, *37*, 21.
2. Zhang, H.; Mittal, G. *Environ. Prog. Sustainable Energy* **2010**, *29*, 203.
3. Lawton, J. W. *Cereal Chem. J.* **2002**, *79*, 1.
4. Goldsmith, B. B. U.S. *patent 922133 (1909)*.
5. Shukla, R.; Cheryan, M. *Indus. Crops Products* **2001**, *13*, 171.
6. Yoshino, T.; Isobe, S.; Maekawa, T. *J. Am. Oil Chemists' Soc.* **2000**, *77*, 699.
7. Soliman, E. A.; Furuta, M. *Radiat. Phys. Chem.* **2009**, *78*, 651.
8. Shi, K.; Kokini, J. L.; Huang, Q. *J. Agricultural Food Chem.* **2009**, *57*, 2186.
9. Rakotonirainy, A. M.; Wang, Q.; Padua, G. W. *J. Food Sci.* **2001**, *66*, 1108.
10. Bai, J.; Alleyne, V.; Hagenmaier, R. D.; Mattheis, J. P.; Baldwin, E. A. *Postharvest Biol. Technol.* **2003**, *28*, 259.
11. Zapata, P. J.; Guillén, F.; Martínez-Romero, D.; Castillo, S.; Valero, D.; Serrano, M. *J. Sci. Food Agriculture* **2008**, *88*, 1287.
12. Niemira, B. A. *Annual Rev. Food Sci. Technol.* **2012**, *3*, 125.
13. Misra, N.; Tiwari, B.; Raghavarao, K. S. M. S.; Cullen, P. *Food Eng. Rev.* **2011**, *1*.
14. Ziuzina, D.; Patil, S.; Cullen, P. J.; Keener, K. M.; Bourke, P. *Food Microbiol.* **2014**, *42*, 109.
15. Pankaj, S. K.; Misra, N. N.; Cullen, P. J. *Innovative Food Sci. Emerging Technol.* **2013**, *19*, 153.
16. Tendero, C.; Tixier, C.; Tristant, P.; Desmaison, J.; Leprince, P. *Spectrochimica Acta Part B: Atomic Spectroscopy* **2006**, *61*, 2.
17. Liu, C.; Cui, N.; Brown, N. M. D.; Meenan, B. J. *Surf. Coat. Technol.* **2004**, *185*, 311.
18. Borcia, G.; Anderson, C. A.; Brown, N. M. D. *Appl. Surf. Sci.* **2004**, *221*, 203.
19. Leroux, F.; Campagne, C.; Perwuelz, A.; Gengembre, L. *J. Colloid Interface Sci.* **2008**, *328*, 412.
20. Ren, C. S.; Wang, K.; Nie, Q. Y.; Wang, D. Z.; Guo, S. H. *Appl. Surf. Sci.* **2008**, *255*, 3421.
21. Kun, W.; Jian, L.; Chunsheng, R.; Dezhen, W.; Younian, W. *Plasma Sci. Technol.* **2008**, *10*, 433.
22. Upadhyay, D. J.; Cui, N.-Y.; Anderson, C. A.; Brown, N. M. D. *Appl. Surf. Sci.* **2004**, *229*, 352.
23. Mastromatteo, M.; Barbuzzi, G.; Conte, A.; Del Nobile, M. A. *Innovative Food Sci. Emerging Technol.* **2009**, *10*, 222.
24. Pereda, M.; Aranguren, M. I.; Marcovich, N. E. *J. Appl. Polym. Sci.* **2009**, *111*, 2777.
25. Pankaj, S. K.; Bueno-Ferrer, C.; Misra, N. N.; O'Neill, L.; Jiménez, A.; Bourke, P.; Cullen, P. J. *J. Renewable Mater.* **2014**, *2*, 77.
26. Akishev, Y.; Grushin, M.; Dyatko, N.; Kochetov, I.; Napartovich, A.; Trushkin, N.; Minh Duc, T.; Descours, S. *J. Phys. D: Appl. Phys.* **2008**, *41*, 235203.
27. Mirabedini, S.; Arabi, H.; Salem, A.; Asiaban, S. *Prog. Organic Coat.* **2007**, *60*, 105.
28. M. C. Almazan-Almazan, J. I. Paredes, M. Perez-Mendoza, M. Domingo-Garcia, F. J. Lopez-Garzon, A. Martinez-Alonso and J. M. Tascon, *J. Colloid Interface Sci.* **2005**, *287*, 57.
29. M. Ataefard, S. Moradian, M. Mirabedini, M. Ebrahimi and S. Asiaban, *Progress in Organic Coatings* **2009**, *64*, 482.
30. Pankaj, S. K.; Bueno-Ferrer, C.; Misra, N. N.; O'Neill, L.; Jiménez, A.; Bourke, P.; Cullen, P. J. *Innovative Food Sci. Emerging Technol.* **2014**, *21*, 107.
31. Lawton, J. W. *Cereal Chem. J.* **2004**, *81*, 1.
32. Wei, W.; Baianu, I. *Macromol. Symp.* **1999**, *140*, 197.
33. Lai, H. M.; Geil, P. H.; Padua, G. W. *J. Appl. Polym. Sci.* **1999**, *71*, 1267.
34. Wang, Y.; Geil, P.; Padua, G. W. *Macromol. Biosci.* **2005**, *5*, 1200.
35. Wang, Y.; Rakotonirainy, A. M.; Padua, G. W. *Starch - Stärke* **2003**, *55*, 25.
36. Singh, N.; Georget, D. M. R.; Belton, P. S.; Barker, S. A. *J. Agric. Food Chem.* **2009**, *57*, 4334.
37. Gao, C.; Stading, M.; Wellner, N.; Parker, M. L.; Noel, T. R.; Mills, E. N. C.; Belton, P. S. *J. Agric. Food Chem.* **2006**, *54*, 4611.
38. Shi, K.; Huang, Y.; Yu, H.; Lee, T. C.; Huang, Q. *J. Agric. Food Chem.* **2010**, *59*, 56.